processes

MDPI

Article

Short-Term Optimal Scheduling of a Cascade Hydro-Photovoltaic System for Maximizing the Expectation of Consumable Electricity

Shuzhe Hu [1], Jinniu Miao [2,*], Jingyang Wu [1], Liqian Zhao [2], Yue Wang [1], Fanyan Meng [3], Chao Wei [1], Xiaoqin Zhang [1] and Benrui Zhu [4]

[1] China Oil & Gas Piping Network Corporation, Beijing 102206, China; m17854262596@163.com (S.H.); miraclejingw@aliyun.com (J.W.); wangyue02@pipechina.com.cn (Y.W.); 18322477717@163.com (C.W.); zhangxq582024@163.com (X.Z.)
[2] China Petroleum Pipeline Engineering Corporation, Langfang 065000, China; zhaoliqian@cnpc.com.cn
[3] China Petroleum Pipeline Research Institute Co., Ltd., Langfang 065000, China; skydream325@163.com
[4] National Key Laboratory of Intelligent Construction and Operation and Maintenance of Water Resources Engineering, Tianjin University, Tianjin 300350, China; benrui.zhu@tju.edu.cn
* Correspondence: 13772187738@163.com

Abstract: Fully leveraging the regulatory role of cascade hydropower in river basins and realizing complementary joint power generation between cascade hydropower and photovoltaic (PV) systems is a crucial approach to promoting the consumption of clean energy. Given the uncertainty of PV outputs, this paper introduces a short-term scheduling model for cascade hydropower–PV systems. The model aims to maximize electricity consumption by considering individual units, hydropower plant constraints, unit constraints, and grid constraints. By allocating loads among hydropower plants and periods, it optimizes hydropower's dual roles, supporting grid power supplies and coordinating with PVs, thus boosting the overall system consumption. In terms of model solution, linearization methods and modeling techniques such as piecewise linear approximation, the introduction of 0–1 integer variables, and the discretization of generation headwater are employed to handle the nonlinear constraints in the original model, transforming it into a mixed-integer linear programming problem. Finally, taking a complementary system constructed by 15 units of 4 hydropower stations and 2 photovoltaic groups in a cascade in a river basin in Southwest China as an example, the results show that through the complementary coordination of cascade hydropower and photovoltaic power, under the same grid constraints, the expected value of the power consumption of the complementary system in the model of this paper increased by 863.2 MW·h, among which the power consumption of photovoltaic group 1 increased by 1035.7 MW·h, and the power consumption of photovoltaic group 2 decreased by 172.5 MW·h.

Keywords: cascade hydropower; complementary system; consumable electricity; mixed-integer linear programming; hydropower plant

check for updates

Academic Editor: Massimo Caruso

Received: 31 December 2024
Revised: 16 January 2025
Accepted: 21 January 2025
Published: 24 January 2025

Citation: Hu, S.; Miao, J.; Wu, J.; Zhao, L.; Wang, Y.; Meng, F.; Wei, C.; Zhang, X.; Zhu, B. Short-Term Optimal Scheduling of a Cascade Hydro-Photovoltaic System for Maximizing the Expectation of Consumable Electricity. *Processes* **2025**, *13*, 328. https://doi.org/10.3390/pr13020328

Copyright: © 2025 by the authors. Licensee MDPI, Basel, Switzerland. This article is an open access article distributed under the terms and conditions of the Creative Commons Attribution (CC BY) license (https://creativecommons.org/licenses/by/4.0/).

1. Introduction

New energy plays an important role in building a new type of power system and realizing the goal of "double carbon". By the end of 2021, China's wind power and photovoltaic installed capacity will be about 635 GW, and it is expected to reach more than 1200 GW in 2030 and 3600 GW in 2050, when the installed capacity of new energy will account for about 70% of the total installed capacity [1]. How to effectively guarantee the

large-scale friendly grid connection and consumption of random and intermittent new energy has brought new challenges to the flexible regulation of the power system.

Building a multi-energy complementary system with wind power and photovoltaics is an important way to solve the flexibility of new energy grid connections. The National Development and Reform Commission's Energy Bureau "on promoting the integration of electric power source network storage and multi-energy complementary development of the guiding opinions" (Development and Reform Energy Regulation (2021) No. 280) clearly puts forward the implementation of a multi-energy complementary path to give full play to basin terrace hydropower plants and has a strong regulating performance of the regulating capacity of hydropower plants to ensure that the comprehensive utilization rate of renewable energy is maintained at a reasonable level [2]. During the "14th Five-Year Plan" period, we will also focus on the development of nine clean energy bases, five of which are related to basin-level hydropower [3]. By the end of 2021, China's installed capacity of hydropower reached 390 GW, forming a cascade hydropower plant group in the basin. According to the latest national water conservancy survey results, there are 98,002 reservoirs with a storage capacity of more than 100,000 m^3, including 756 large reservoirs and 3938 medium reservoirs [4]. Such a huge "energy storage" system provides a good foundation for realizing the multi-energy complementarity of solar and new energy sources.

At present, regarding the multi-energy complementarity of hydropower, photovoltaic and other new energy sources, in addition to the capacity planning and the design of the complementary system [5–7], its operation scheduling has also received extensive attention [8]. In [9], the scheduling model of a water–photovoltaic complementary system was constructed based on different control strategies of minimum total output fluctuations and the optimal overall stationarity. In [10], considering the randomness of photovoltaic output, an operation safety analysis method based on a probabilistic collocation algorithm based on polynomial chaos theory is proposed, which provides theoretical support for the safe and stable operation of a cascade water–photovoltaic complementary system. In [11], considering the short-term volatility of photovoltaics, a medium- and long-term optimal scheduling method of a water–photovoltaic complementary system with nested short-term power abandonment risks was proposed. Ref. [12] established a short-term optimal scheduling model of water–photovoltaic complementarity in Longyang Gorge and analyzed the water–photovoltaic complementarity effect under various scenarios. Based on the photovoltaic energy loss function, [13] established a relationship between short-term and long-term scheduling models and proposed an adaptive operating rule for water–photovoltaic complementary systems. Ref. [14] established a dual-objective scheduling model that took into account power generation and output fluctuations and reduced PV output fluctuations on the premise of ensuring power generation. Ref. [15] constructed a short-term optimal scheduling model of a cascade water–photovoltaic-combined power generation system with the goal of minimizing the water consumption of cascade hydropower. According to comprehensive investigations and analyses, the essence of water–photovoltaic complementarity is to give play to the good regulation ability of hydropower to promote the absorption of random photovoltaics, and this research mainly focuses on complementary characteristics analysis, output fluctuation reduction, operation safety analysis, and other aspects. Most of the existing models take the hydropower plant as the minimum dispatching unit and do not carefully consider the complex operational constraints of the unit and the grid, which makes the implementation of the plan of each hydropower plant biased and even difficult to execute. For example, the same hydropower plant may contain multiple units of different types, and different types of units have different climbing capacities, vibration zones, start–stop times, and other constraints and cannot be generalized. Ref. [16] discusses the technical challenges and operational constraints associated with integrating

large-scale hydropower facilities into a grid, highlighting the importance of transmission section capacity planning. Conversely, ref. [17] delves into the economic and regulatory aspects of cascading hydropower development, emphasizing the need for coordinated grid integration strategies to optimize energy dispatch and minimize transmission bottlenecks. In addition, smoothing out the volatility of photovoltaics may lead to frequent fluctuations of hydropower outputs, causing losses and operational risks to hydropower units [18–20]. The research of [18] analyzes the technical challenges associated with integrating PV and hydropower systems, emphasizing how PV variability can impact hydropower operations and output stability. Ref. [19] delves into the economic implications of these fluctuations, highlighting the potential for financial losses and increased operational costs due to the unpredictability of PV power generation. Lastly, ref. [20] explores the regulatory and policy frameworks necessary to address these challenges, suggesting strategies for optimizing the integration of PVs and hydropower to minimize negative impacts on hydropower units. How to avoid frequent fluctuations of hydropower outputs in complementary scheduling is also a problem that needs to be considered.

Therefore, on the basis of previous studies, this paper takes the unit as the minimum dispatching unit, uses the fuzzy clustering method to construct the output scenario to describe PV uncertainty, and carefully considers the constraints of the hydropower plant, the unit, and the grid faced by the complementary system and constructs a short-term optimal scheduling model to maximize the expectation of the consumed power of the cascade water–photovoltaic complementary system. Through the reasonable allocation of cascade loads in hydropower plants and periods, the dual role of cascade hydropower in the power supply support and photovoltaic complementary regulation of power grids is explored to improve the overall power consumption level of the complementary system.

The proposed model is a high-dimensional multi-variable, multi-reduced bundle hybrid integer nonlinear programming (MINLP) problem, which has been solved by intelligent algorithms in several studies. The quality of the solution is greatly affected by the initial solution, and it is easy to fall into the local optimal solution, and it is difficult to ensure convergence to the global optimal solution. With the development of commercial solution tools in recent years, mixed-integer linear programming (MILP) has been widely used in the field of hydropower due to its advantages such as a mature algorithm, high solution efficiency, and stable results [21–24]. In order to realize the efficient solution of the model, for the nonlinear constraints involved in the model, piecewise linear approximation, the introduction of 0–1 integer variables, power generation head discretization, and other linearization methods and modeling skills are used to transform the original MINLP problem into an MILP problem, and the CPLEX tool is used to solve the problem. Finally, taking 15 units of 4 hydropower plants and 2 PV clusters in a river basin in Southwest China as a reference, a complementary system is constructed to verify the effectiveness of the model and solution method proposed in this paper.

2. Materials and Methods

2.1. Objective Function

Considering the uncertainty of PV outputs, with the objective of maximizing the expected amount of power that can be consumed by a cascade hydropower–PV complementary system, the following function can be expressed:

$$F = \max \sum_{s=1}^{s} \{\mathrm{Prob}(s)[\sum_{t=1}^{T}(\sum_{i=1}^{I} P_{i,t}^{\mathrm{hydro}} + \sum_{j=1}^{J} P_{j,t}^{\mathrm{pv}}(r_{s,j}) - \sum_{g=1}^{G} P_{g,t}^{\mathrm{w}}(s))\Delta t]\} \quad (1)$$

where $S = \prod_{j=1}^{J} S_j$ is the combined field size of the PV station output; $\text{Prob}(s) = \prod_{j=1}^{J} p(r_{s,j})$ is the occurrence probability of the s-th output combination scenario; $r_{s,j}$ and $p(r_{s,j})$ are the corresponding scenario to which PV station j belongs in the s-th combination scenario and the probability of this scenario, respectively. And satisfy $1 \leq r_{s,j} \leq S_j$. $P_{i,t}^{\text{hydro}}$ represents the output of the hydropower plant i at time t, $P_{j,t}^{\text{pv}}(r_{s,j})$ represents the output of the PV station j in scenario $r_{s,j}$ at time t, and $P_{g,t}^{\text{w}}(s)$ represents the amount of curtailed electricity for the gth constraint section in scenario s at time t. I, J, G, and T represent the total number of hydropower plants, the total number of photovoltaic fields, the number of constrained sections, and the total number of periods. Δt represents the number of hours in a single period.

2.2. Constraint Condition

The constraints include various types of power plant constraints, unit constraints, and grid constraints, as follows:

2.2.1. Hydropower Plant Constraint

(1) Water balance constraint

$$V_{i,t} = V_{i,t-1} + 3600(I_{i,t} - Q_{i,t})\Delta t \tag{2}$$

$$I_{i,t} = Q_{i-1,t-\tau} + R_{i,t} \tag{3}$$

$$Q_{i,t} = Q_{i,t}^{\text{p}} + Q_{i,t}^{\text{d}} \tag{4}$$

where $V_{i,t}$ is the storage capacity of the hydropower plant i at the end of time t; $I_{i,t}$ is the incoming storage flow of the hydropower plant i; τ is the time of water flow stagnation between station i and its upstream station i-1; $Q_{i,t}$ is the outbound flow of the hydropower plant i; $Q_{i\text{-}1,t\text{-}\tau}$ is the flow rate of the hydropower plant i-1 in the t-τ period after considering water stagnation; $R_{i,t}$ is the interval flow between the hydropower plant i-1 and the hydropower plant i; $Q_{i,t}^{\text{p}}$ and $Q_{i,t}^{\text{d}}$ are the generation flow and waste water flow of the hydropower plant i, respectively.

(2) Reservoir-level constraint

$$\underline{Z}_{i,t}^{\text{up}} \leqslant Z_{i,t}^{\text{up}} \leqslant \overline{Z}_{i,t}^{\text{up}} \tag{5}$$

where $Z_{i,t}$, $\overline{Z}_{i,t}^{\text{up}}$, and $\underline{Z}_{i,t}$ are, respectively, the water level in front of the dam and its upper and lower limits of the reservoir where the hydropower plant i is located at time t.

(3) Initial and final water level control

$$Z_{i,1}^{\text{up}} = Z_{i,\text{begin}}^{\text{up}} \tag{6}$$

$$\left| Z_{i,T}^{\text{up}} - Z_{i,\text{end}}^{\text{up}} \right| \leqslant \Delta Z \tag{7}$$

where $Z_{i,\text{begin}}^{\text{up}}$ and $Z_{i,\text{end}}^{\text{up}}$ are the initial water level and the control water level at the end of the scheduling period, respectively, and ΔZ is the allowable deviation of the water level at the end of the dispatch period to avoid affecting the water volume of the next dispatch cycle.

(4) Outbound traffic constraints

$$\underline{Q}_{i,t} \leqslant Q_{i,t} \leqslant \overline{Q}_{i,t} \tag{8}$$

where $\overline{Q}_{i,t}$ and $\underline{Q}_{i,t}$ are, respectively, the upper and lower limits of the outgoing storage flow of the hydropower plant i.

(5) Hydropower plant output constraint

$$\underline{P}_{i,t}^{\text{hydro}} \leqslant P_{i,t}^{\text{hydro}} \leqslant \overline{P}_{i,t}^{\text{hydro}} \tag{9}$$

where $\overline{P}_{i,t}^{\text{hydro}}$ and $\underline{P}_{i,t}^{\text{hydro}}$ are, respectively, the upper and lower limits of the output of the hydropower plant i.

(6) Water level–storage relationship

$$V_{i,t} = f_i^{\text{zv}}\left(Z_{i,t}^{\text{up}}\right) \tag{10}$$

where $f_i^{\text{zv}}(\cdot)$ is the nonlinear relation curve function of the water level and storage capacity of the reservoir where the hydropower plant i is located.

(7) Tail water–discharge relationship

$$Z_{i,t}^{\text{down}} = f_i^{\text{zq}}(Q_{i,t}) \tag{11}$$

where $f_i^{\text{zq}}(\cdot)$ is the nonlinear curve function of the relationship between the tail water level of the hydropower plant i and the discharge rate, and $Z_{i,t}^{\text{down}}$ is the tail water level of the hydropower plant i.

2.2.2. Unit Constraint

(1) Unit output constraint

$$u_{i,n,t}\underline{P}_{i,n} \leqslant P_{i,n,t} \leqslant u_{i,n,t}\overline{P}_{i,n} \tag{12}$$

where $P_{i,n,t}$, $\overline{P}_{i,n}$, and $\underline{P}_{i,n}$ are, respectively, the output of the n-th unit of the hydropower plant i at time t and its upper and lower limits; $u_{i,n,t}$ is the on/off state variable of the n-th unit of the power plant i at time t; $u_{i,n,t} \in \{0,1\}$, with 1 meaning the on state and 0 meaning the off state. Therefore, the output of each hydropower plant i can be expressed as follows:

$$P_{i,t}^{\text{hydro}} = \sum_{n=1}^{N_i} u_{i,n,t}P_{i,n,t} \tag{13}$$

where N_i is the total number of units contained in the hydropower plant i.

(2) Constraints on generating the flow of the unit

$$u_{i,n,t}\underline{Q}_{i,n}^{\text{p}} \leqslant Q_{i,n,t}^{\text{p}} \leqslant u_{i,n,t}\overline{Q}_{i,n}^{\text{p}} \tag{14}$$

where $Q_{i,n,t}^{\text{p}}$, $\overline{Q}_{i,n}^{\text{p}}$, $\underline{Q}_{i,n}^{\text{p}}$ represent the power generation flow of the n-th unit of the hydropower plant i during time t, along with its upper and lower limits. Therefore, the power generation flow for each hydropower plant i can be expressed as follows:

$$Q_{i,t}^{\text{p}} = \sum_{n=1}^{N_t} u_{i,n,t}Q_{i,n,t}^{\text{p}} \tag{15}$$

(3) Unit vibration zone constraints

$$(P_{i,n,t} - P_{i,n,k}^{\max})(P_{i,n,t} - P_{i,n,k}^{\min}) \geqslant 0 \tag{16}$$

where $P_{i,n,k}^{\max}$ and $P_{i,n,k}^{\min}$ are the upper and lower limit of the output in the k vibration zone of the n-th unit of the hydropower plant i.

(4) Unit on and off duration constraints

$$\begin{cases} u_{i,n,t} - u_{i,n,t-1} = y_{i,n,t}^{\text{on}} - y_{i,n,t}^{\text{off}} \\ y_{i,n,t}^{\text{on}} + y_{i,n,t}^{\text{off}} \leqslant 1 \\ y_{i,n,t}^{\text{on}} + \sum\limits_{\lambda=t+1}^{t+T_{i,n}^{\text{on}}-1} y_{i,n,\lambda}^{\text{off}} \leqslant 1 \\ y_{i,n,t}^{\text{off}} + \sum\limits_{\lambda=t+1}^{t+T_{i,n}^{\text{off}}-1} y_{i,n,\lambda}^{\text{on}} \leqslant 1 \\ \sum\limits_{t=1}^{T} y_{i,n,t}^{\text{on}} \leqslant M_{i,n}^{\text{on}} \end{cases} \tag{17}$$

where $y_{i,n,t}^{\text{on}} \in \{0,1\}$ is the startup operation variable of the n-th unit of the hydropower plant i at time t, and 1 represents the startup operation; $y_{i,n,t}^{\text{on}} \in \{0,1\}$ represents the shutdown operation of the n-th unit of the hydropower plant i during time t, where a value of 1 indicates that a shutdown operation is occurring. $T_{i,n}^{\text{on}}$ and $T_{i,n}^{off}$ represent the minimum startup and shutdown duration of the n-th unit of the hydropower plant i. The maximum number of startups for the n-th unit of the hydropower plant i during the scheduling time is $M_{i,n}^{\text{on}}$, in order to avoid frequent shutdowns and restarts.

(5) Unit output climbing constraints

$$-\Delta P_{i,n} \leqslant P_{i,n,t+1} - P_{i,n,t} \leqslant \Delta P_{i,n} \tag{18}$$

where $\Delta P_{i,n}$ is the climbing capacity of the n-th unit of the hydropower plant i.

(6) Unit output fluctuation restriction

$$\begin{gathered} (P_{i,n,t} - P_{i,n,t-\sigma-1})(P_{i,n,t} - P_{i,n,t-1}) \geqslant 0 \\ \sigma = 1, 2, \cdots, t_{\text{e}} - 1 \end{gathered} \tag{19}$$

where t_{e} is the minimum duration of the unit in the process of a round of output rises and falls, $t_{\text{e}} > 1$. This constraint not only reduces the loss of frequent adjustments of the unit, but more importantly, it can reduce the frequent fluctuation of the discharged flow, which is conducive to ensuring the stability of the ecological flow.

(7) Power generation head constraints

$$H_{i,n,t} = \frac{Z_{i,t}^{\text{up}} - Z_{i,t-1}^{\text{up}}}{2} - Z_{i,t}^{\text{down}} - H_{i,n,t}^{\text{loss}} \tag{20}$$

where $H_{i,n,t}$ and $H_{i,n,t}^{\text{loss}}$ are the power generation head and head loss of the n-th unit of the hydropower plant i at time t, respectively.

(8) Head loss function

$$H_{i,n,t}^{\text{loss}} = a_i (Q_{i,n,t}^{\text{p}})^2 + b_i \tag{21}$$

where a_i and b_i are head loss coefficients and loss constants of the hydropower plant i, which can generally be obtained through hydraulic tests.

(9) Relationship of unit power characteristics

$$P_{i,n,t} = f_{i,n}^{\text{OHF}}(Q_{i,n,t}^{\text{p}}, H_{i,n,t}) \tag{22}$$

where $f_{i,n}^{\text{OHF}}(\cdot)$ is the nonlinear relationship function of output–head-flow for the n-th unit of the hydropower plant i.

2.2.3. Grid Constraints

(1) Constraints on the range of cascade hydropower output

$$\left| \sum_{i=1}^{I} P_{i,t}^{\text{hydro}} - P_t^{\text{plan}} \right| \leqslant \varepsilon \ \forall t = 1, 2, \cdots, T \tag{23}$$

where P_t^{plan} is the power generation plan of the cascade hydropower, which constrains the range of the cascade output within the permitted reasonable deviation ε and ensures the power supply support capability of the cascade hydropower to the power grid from the perspective of the balance of electric power and the stability of the power supply.

(2) Sectional section constraint

$$P_{g,t}^{\text{w}}(s) = \max(P_{s,g,t} - L_{g,t} - C_{g,t}, 0) \tag{24}$$

$$P_{s,g,t} = \sum_{n,j \in \Omega_s} (P_{i,n,t} + P_{j,t}^{\text{pv}}(r_{s,j})) \tag{25}$$

where $L_{g,t}$ and $C_{g,t}$ are, respectively, the upper limit of the load and transmission capacity of the g-constrained section at time t. $P_{s,g,t}$ is the total output of all units at time t under the g-constrained section of the s-type combination scenario. Ω_g is a collection of hydropower units and photovoltaic fields under the g-constrained section.

From the objective function and zonal section constraints, it can be seen that abandoned power is not set in abandoned water, prioritizing abandoned photovoltaics. The model objective will make the gradient hydropower be in the permitted range of output-priority water storage and will reduce the hair in order to enhance the amount of photovoltaic consumption in the obstructed section, so as to enhance the overall level of the complementary system that can be consumed and in order to ensure that the power supply that supports the power grid does not continue to reduce the hair by the zonal section limitations caused by the abandonment of photovoltaics, which is also unavoidable.

2.3. Model Transformation

The key to MILP model construction lies in the linearization transformation of the model, and the nonlinear constraints of the proposed model include Equations (10), (11), (16), (19), (21), and (22). Among these, the water level–capacity, tail water level–discharge flow rate, and head loss functions can be handled in a segmented linear way [21]. The dynamic characteristics of the machine group are referred to in [22] and were processed by the triangular weight technique. In particular, for seasonal regulation and above hydropower plants, the variation of water levels at the beginning and end of the day is small, and a linear function can be used to show the relationship between water level and reservoir capacity near the initial water level.

(1) Constrained linearization of the unit vibration zone

Multiple vibration zones may exist in large units, dividing the output into multiple non-contiguous safe operating intervals within the maximum and minimum output ranges. Drawing on [21], this paper assumes that the vibration zone of the unit does not change with a change in the unit head, i.e., a fixed vibration zone, and assuming that the unit has K vibration zones, there are K + 1 safe operation intervals, namely, the following:

$$[\underline{P}_{i,n}, P_{i,n,1}^{\min}], \cdots, [P_{i,n,k-1}^{\max}, P_{i,n,k}^{\min}], [P_{i,n,k}^{\max}, \overline{P}_{i,n}] \tag{26}$$

The 0–1 variable $\theta_{i,n,t,k}$ is introduced to denote the safety interval in which the outgoing force is located, and the linearization is treated as follows:

$$\sum_{k=1}^{K+1} \theta_{i,n,t,k} P_{i,n,k-1}^{\max} \leqslant P_{i,n,t} \leqslant \sum_{k=1}^{K+1} \theta_{i,n,t,k} P_{i,n,k}^{\min} \tag{27}$$

$$\sum_{k=1}^{K+1} \theta_{i,n,t,k} = u_{i,n,t} \tag{28}$$

where $\theta_{i,n,t,k}$ is the vibration zone indicator variable, which is taken as 1 to indicate that the n-th unit of the power plant i is in the k-th safe operation interval at time t. Therefore, it is not necessary for the n-th unit of the power plant i to be in the k-th safe operation interval. Therefore, the nonlinear constraint in Equation (16) can be replaced by Equations (26)–(28).

(2) Linearization of hydroelectric unit output fluctuation limitation constraints

Frequent fluctuations in hydroelectric unit outputs are manifested as an upward or downward regulation of the output in neighboring periods. Different from the methods of correlation searches [23] and load reconstructions [24] adopted in the existing literature, this paper innovatively handles the problem by introducing regulation indicator variables, which can effectively improve the solution efficiency.

$$-\alpha_{i,n,t} \Delta P_{i,n} \leqslant P_{i,n,t+1} - P_{i,n,t} \leqslant \beta_{i,n,t} \Delta P_{i,n} \tag{29}$$

$$\begin{cases} \alpha_{i,n,t} + \beta_{i,n,t} \leqslant 1 \\ \sum\limits_{t=1}^{T} (\alpha_{i,n,t} + \beta_{i,n,t}) \leqslant M_{a\beta} \end{cases} \tag{30}$$

where $\alpha_{i,n,t} \in \{0,1\}$ and $\beta_{i,n,t} \in \{0,1\}$ are the power adjustment index variables of the n-th unit of the hydropower plant i at time t, $\alpha_{i,n,t} = 1$ indicates that the power is adjusted downward at time $t+1$, and $\beta_{i,n,t} = 1$ indicates that the power is adjusted upward at time $t+1$. When the power does not change, $\alpha_{i,n,t} = 0$ and $\beta_{i,n,t} = 0$, and $M_{\alpha\beta}$ is the upper limit of the number of periods for power adjustments (upward and downward).

In addition, the following constraints are introduced to ensure that the unit is able to maintain a stable output for at least a certain amount of time t_e after each output adjustment:

$$\begin{cases} \alpha_{i,n,t} + \beta_{i,n,t+t_s} \leqslant 1 \\ \beta_{i,n,t} + \alpha_{i,n,t+t_s} \leqslant 1 \\ \sum\limits_{\gamma=0}^{t_s} \alpha_{i,n,t+\gamma} \leqslant 1 \ \ \forall t_s = 1, 2, \cdots, t_e - 1 \\ \sum\limits_{\gamma=0}^{t_s} \beta_{i,n,t+\gamma} \leqslant 1 \end{cases} \tag{31}$$

Therefore, the nonlinear approximate bundle of Equation (19) can be replaced by Equations (29)–(31). Figure 1 shows a schematic diagram of the state change of the unit. When the stable output time of the unit reaches t_e, the unit has three effective states of up, down, and stable outputs. Suppose that this is t_0. If the output is up or down at t_1, only the stable output state is effective after an adjustment, and the up and down state is temporarily invalid. Until the stable output time reaches t_e again, the up and down state of the unit is effective again, so that the stability of the unit's output is guaranteed by period constraints.

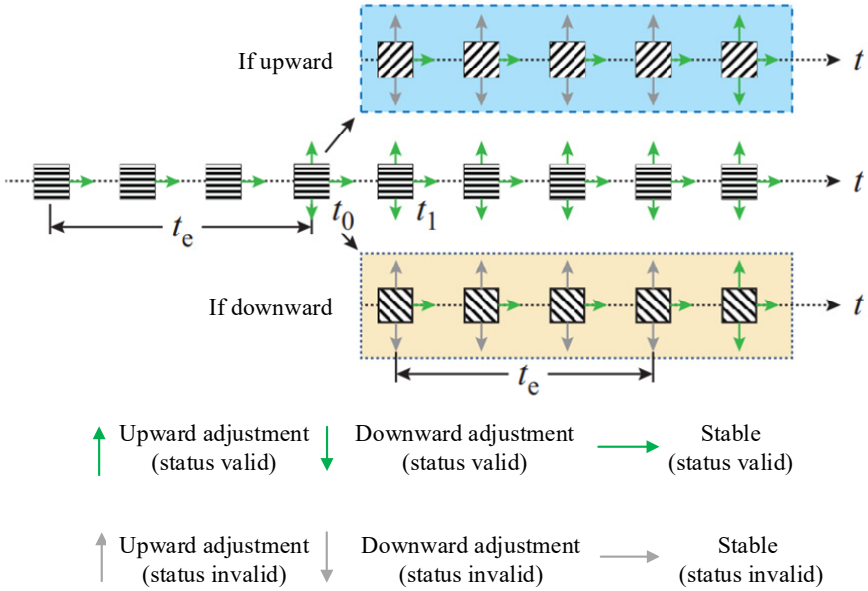


Figure 1. Schematic diagram of up and down regulation status of hydropower unit output.

2.4. Photovoltaic Output Scenario Construction

Influenced by weather changes, forecasting methods, and other factors, the deviation between a PV-forecasted output and an actual output exists objectively. In this paper, the historical deviation data are taken as samples, and fuzzy clustering analysis is used to construct PV output scenarios, and the specific method flow is as follows.

(1) Discharge deviation treatment

$$\Delta P_{j,t}^{\mathrm{pv}} = \frac{P_{j,t}^{\mathrm{pv}} - P_{j,t}^{\mathrm{pv}^*}}{N_j^{\mathrm{pv}}} \tag{32}$$

where $\Delta P_{j,t}^{\mathrm{pv}}$, $P_{j,t}^{\mathrm{pv}}$, and $P_{j,t}^{\mathrm{pv}^*}$ are the predicted deviation, predicted output, and actual output of the PV field j at time t, respectively, and N_j^{pv} is the installed capacity of the PV field j.

(2) Fuzzy cluster analysis

The deviation curve of the predicted output and actual output at 96 points within the historical days of PV stations was taken as a sample, and fuzzy clustering analysis was carried out, and the integrated quality of the clustering was used to determine the optimal number of clusters, and finally, the fuzzy clustering centers of each category were used to construct the predicted output deviation scenarios, and the specific formulas and detailed steps can be found in [25].

(3) PV output scenarios

The predicted output deviation of the PV field j under scenario $r_{s,j}$ was obtained from Equation (32) and is denoted as follows:

$$\Delta P_j^{\mathrm{pv}}(r_{s,j}) = \left\{ \Delta P_{j,1}^{\mathrm{pv}}(r_{s,j}), \Delta P_{j,2}^{\mathrm{pv}}(r_{s,j}), \cdots, \Delta P_{j,T}^{\mathrm{pv}}(r_{s,j}) \right\} \tag{33}$$

Then, the output curve at scene $r_{s,j}$ is as follows:

$$P_{j,t}^{\mathrm{pv}}(r_{s,j}) = P_{j,t}^{\mathrm{pv}} - N_j^{\mathrm{pv}} \Delta P_{j,t}^{\mathrm{pv}}(r_{s,j}) \tag{34}$$

The corresponding probability can be obtained from the ratio of the number of samples belonging to scenario $r_{s,j}$ to the total number of samples.

2.5. Solution Process

The steps for solving the expectation model for maximizing the consumable power of the complementary system described in this paper are as follows:

Step 1: read the basic data and set the calculation conditions, including the interval flow, step generation plan, PV-predicted output, PV historical prediction and actual output, zoning section constraints, climbing capacity, etc.

Step 2: Model conversion processing: adopt the model conversion method described in Section 2.1 to linearize the nonlinear constraints.

Step 3: Construction of PV output scenarios: construct the PV output scenario according to the predicted PV output on the planned day and the method described in Section 2.2.

Step 4: Model solving: Combine the objective function with the transformed constraints to form the MILP model, and in the environment, encode and call the CPLEX solver class to realize the model solving. Algorithm coding examples can be found in Appendix A.

Step 5: Output: Output the expected value of the overall power consumption of the complementary system, and the resulting information of the power plant output, unit output, unit start and stop, outgoing flow, and reservoir level under different combination scenarios.

3. Results and Discussion

3.1. Engineering Background

A complementary system constructed by 4 hydropower plants with 15 units and two PV groups in a basin terrace in Southwest China was used as the research object to verify the effectiveness of the model and the solution method proposed in this paper, and the simplified terrace hydrodynamic relationship and the network topology are shown in Figure 2. Typical daily scenarios were selected during the dry season, with 1 d as the dispatch cycle and 15 min as the dispatch period, and the power generation plan of the gradient hydropower plants, as well as the predicted output of PVs, and the grid parameters were all set with reference to the actual situation of the power grid.

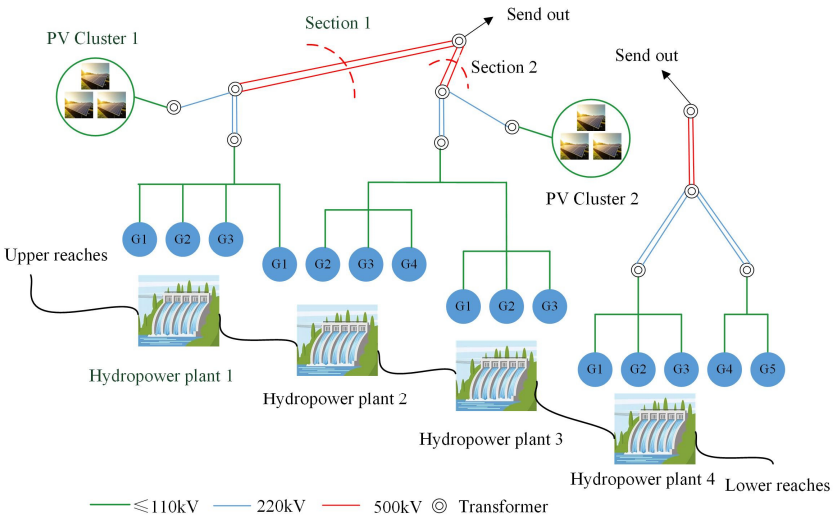


Figure 2. Schematic diagram of cascade hydraulic relation and grid topology.

The characteristic parameters of each hydropower plant in the hierarchy and the zonal transmission constraints are shown in Tables 1 and 2, respectively. Other model parameters were set as follows: $\Delta P_{i,n}$ was 60 MW/15 min; the number of stable output limitation periods t_e was 4, i.e., 1 h; the upper limit of power adjustment periods $M_{\alpha\beta}$ was 12; and the allowable deviation ε of the ladder generation plan ε was 2%.

Table 1. Main characteristic parameters of cascade hydropower plant.

Hydropower Plant Number	Adjustment Performance	Unit Number	Single Unit Capacity/MW	Vibration Zone/MW	Unit Start/Stop Duration/h	Duration of Stabilized Output/h	Water Flow Stagnation Time/h
1	Multi-year conditioning	1, 2, 3	200	(45, 90)	2	1	
2	Seasonal adjustments	1, 2, 3, 4	190 125	(40, 110) (30, 80)	2 2	1 1	1
3	Daily regulations	1, 2, 3	200	(0, 130)	2	1	2
4	Incomplete annual reconciliation	1, 2, 3, 4, 5	250 250	(50, 70) and (80, 90) (30, 80) and (140, 170)	2 2	1 1	1

Table 2. Transmission capacity limitation of different sections.

Section Number	Voltage Level/kV	Includes Cascade Hydropower Plants and Units		Capacity Limit/MW
		Hydropower Plant	Unit Number	
1	500	1 2	1, 2, 3 1	900
2	500	2 3	2, 3, 4 1, 2, 3	1500
3 4	220 220	4 4	1, 2, 3 4, 5	750 500

3.2. Analysis of Results

In the modeling, the outflow of hydropower units (including power generation flow and water disposal flow) was used as the decision variables, with 96 periods and 2880 decision variables in total. The convergence accuracy of the model was set to 10^{-4} after several tests.

3.2.1. PV Power Output Scenario Analysis

Taking the day-by-day 96-point predicted output and actual output data from January 2015 to December 2021 as samples, PV output scenarios were constructed in accordance with the methods and processes described in Section 3.2. Taking PV cluster 1 as an example, the weather forecast was cloudy a few days ago, and the optimal number of clusters was determined to be 4 by the cluster synthesis quality method, and the probabilities of the four output scenarios are 25%, 17%, 39%, and 19%, respectively. PV cluster 2 was analyzed similarly, resulting in a total of 16 PV output mix scenarios, as shown in Figure 3.

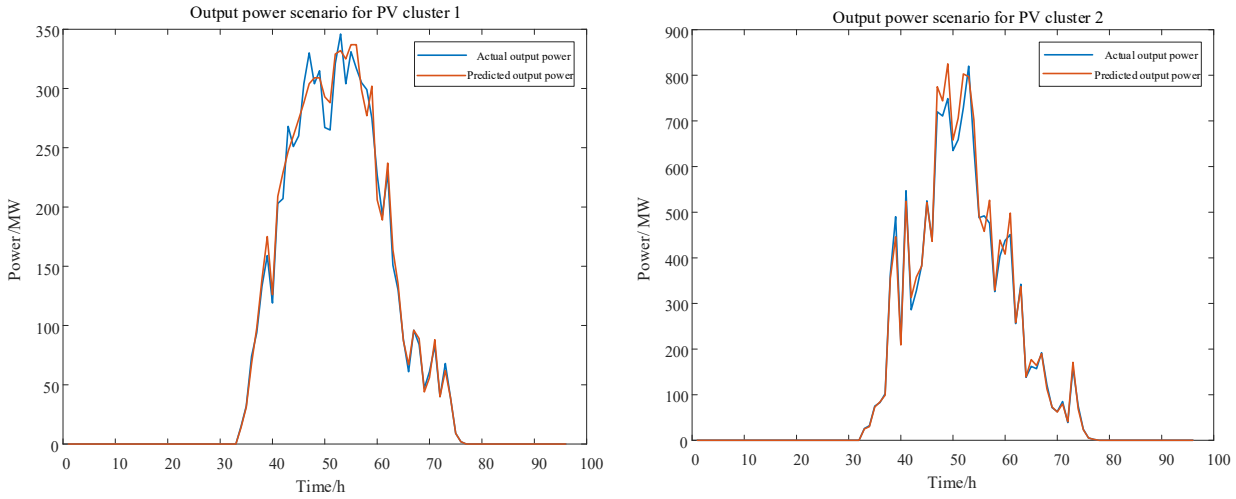


Figure 3. Output scenarios of photovoltaic cluster 1 and 2.

3.2.2. Analysis of the on and off State of Hydropower Plants

The model in this paper takes the unit as the minimum dispatching unit and can directly obtain the on–off state of the hydropower unit under different PV output scenarios. Hydropower plant 2 has seasonal adjustment performance and intraday adjustment abilities, and unit 1 and units 2 to 4 belong to Sections 1 and 2 and participate in the complementary coordination degree of photovoltaics. During the day, basically, 4 units are kept on, which can ensure the power supply support for the grid, and the complementary coordination of photovoltaic outputs in different combination scenarios is met. During the night low period, the main two units are turned on to meet the cascade load requirements during the low period when the PV output is 0. In some combination scenarios, due to the large PV prediction deviation, three units are required to be turned on to provide greater adjustment space. There is no photovoltaic in the section of hydropower plant 3 and hydropower plant 4, and the complementary adjustment ability of directly participating in photovoltaics is weak. They should bear the cascade load as far as possible within the section constraints, and the units should be started all the time to make more adjustment space for hydropower plants 1 and 2. The optimal operating number of units for each hydropower plant is shown in Table 3.

Table 3. The optimal number of units for each hydropower plant.

Hydropower Plant	Optimal Operating Number
1	3
2	4
3	3
4	4

3.2.3. Cascade Hydropower Results Analysis

Taking the scenario of a maximum probability combination as an example, the results of the cascade hydropower calculation were analyzed.

(1) Power output process of cascade hydropower plants

The output process of cascade hydropower plant is shown in Figure 4. The average deviation between the actual output process of cascade hydropower and the given cascade power generation plan is 1.92%, which meets the deviation requirement, and the power supply support function of the grid is reliable. From the point of view of the output process, the output of each hydropower plant is stable and does not fluctuate frequently after considering the constraints of unit start–stops and fluctuation durations, which meets the actual operation requirements of the hydropower plant.

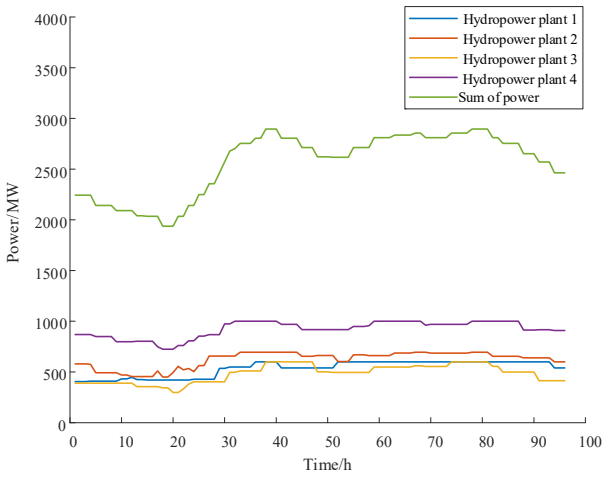


Figure 4. Power output process of different cascade hydropower plants.

(2) Hydropower unit power output process

The power output process of some hydropower units is shown in Figure 5. It can be seen that the output of each unit effectively avoids the vibration zone and meets the constraint requirements of the unit's climbing capacity, ensuring the safety of operations. At the same time, the stable output duration of the unit meets the requirements of the output fluctuation limit constraint (1 h), and the start–stop duration constraint also meets the minimum start–stop duration of the unit for 2 h, ensuring the stability of the unit output. Therefore, the validity of the constraint processing method proposed in this paper was verified.

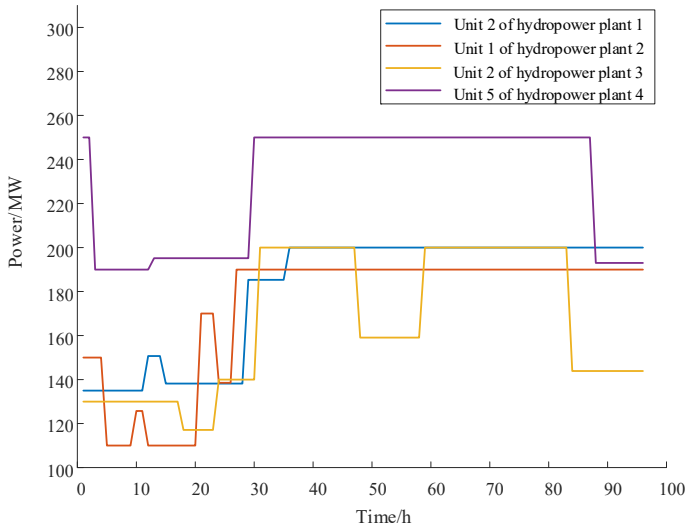


Figure 5. Power output process of some hydropower units.

(3) Water level process of hydropower plant

Considering the small intraday water level fluctuations of the hydropower plant with seasonal adjustments and above, taking hydropower plant 3 as an example, the variation process of intraday water levels is given, as shown in Figure 6. It can be seen that the intraday water level of the daily regulating hydropower plant fluctuates greatly, with a maximum amplitude of 0.46 m. If the traditional method describes the water–storage relationship and head loss with a simple linear relationship near the water level at the beginning of the period, there will be a large deviation. The method of piecewise linearization was adopted in this paper, which can effectively avoid the influence of this part and is more in line with the actual operation.

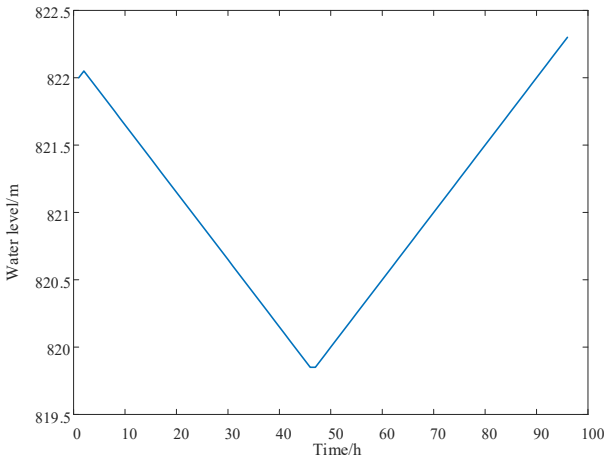


Figure 6. Upstream level of hydropower plant 3.

(4) Output analysis of each section

The output process of each section is shown in Figure 7. Taking Section 1 as an example, the output and power abandonment under this section were analyzed. This section includes units 1 to 3 of hydropower plant 1, unit 1 of hydropower plant 2, and photovoltaic group 1. It can be seen that Section 1 has abandoned electricity during part of the peak period of photovoltaic output from 10:00 to 15:00. Through an analysis of reasons for this, it can be seen that through the complementary coordination of cascade hydropower to PV, the maximum absorption of PVs in the section is promoted, and the overall absorption level of the complementary system is improved. However, cascade hydropower is limited by its own hydraulic and electrical constraints, and the promotion ability is limited when the power supply support of the grid is given priority, which inevitably causes the abandonment of photovoltaics. Section 1 is similar to Section 2, and there is no photovoltaic in Sections 3 and 4. During the peak hours of photovoltaic output, the channel is fully used to send out the cascade load, providing more adjustment space for the hydropower plant under Sections 1 and 2.

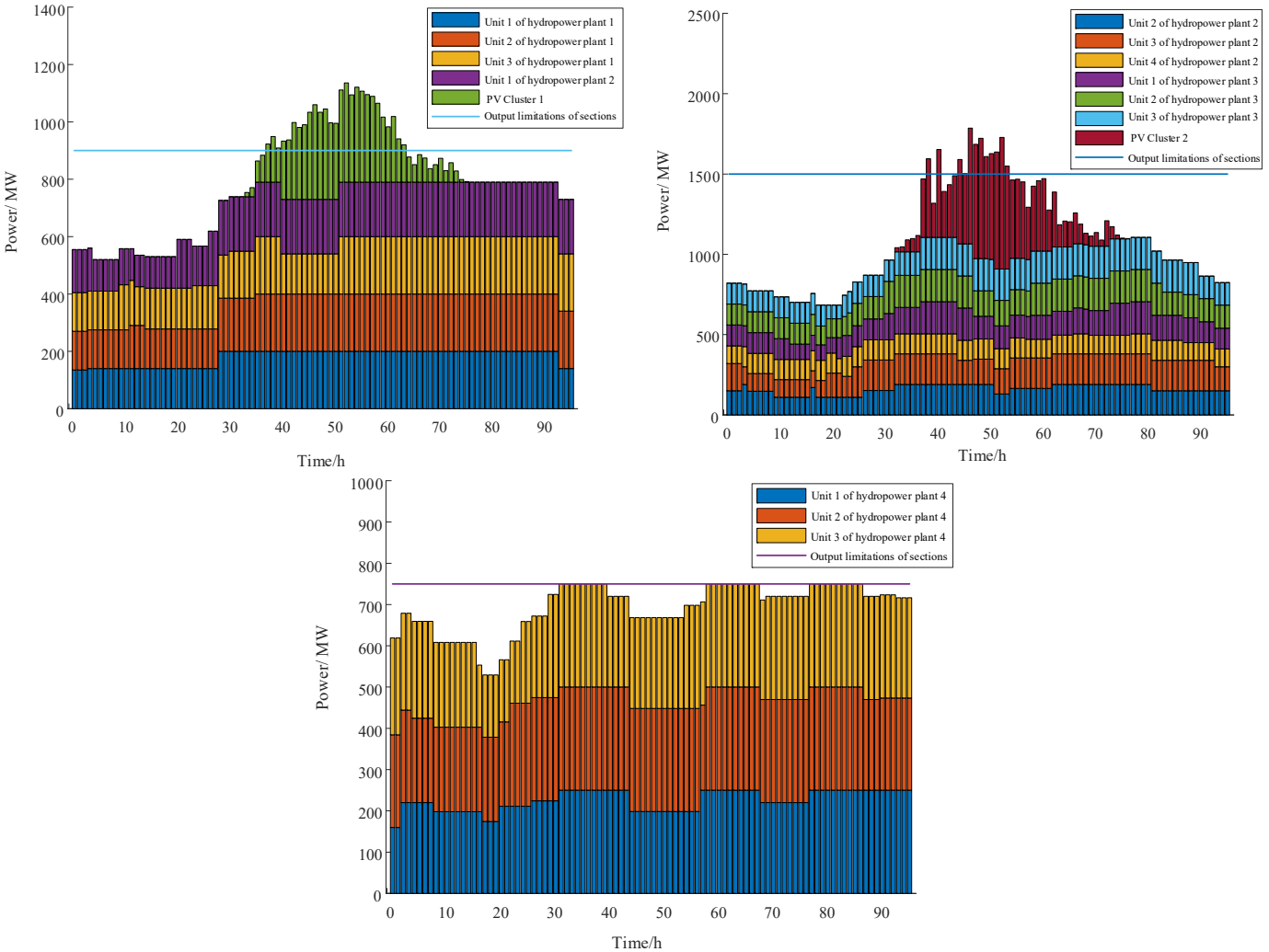


Figure 7. Power output process of each section.

3.2.4. Comparative Analysis of Complementary Effects

In order to verify the complementarity effects of cascade hydropower and photovoltaics under the model proposed in this paper, assuming that cascade hydropower operates independently and does not participate in PV complementarity and considering

only its own costs and benefits, a comparison model was constructed with the goal of minimum water consumption under a given cascade load (the same cascade load as the model proposed in this paper). The comparison results of the model are shown in Table 4.

Table 4. Result comparison of different models.

Model	Expectation of the Amount of Electricity that Can Be Consumed/(MW·h)				Amount of Electricity Discarded/(MW·h)	Water Consumption/Million m^3	Water Consumption Rate/$(m^3 \cdot (kW \cdot h)^{-1})$
	Cascade Hydropower Plant	PV Cluster 1	Photovoltaic Group 2	Total			
Text model	61,440.2	2306.53	4586.54	68,333.25	290.15	23,503.29	3.82
Comparison model	61,440.2	1270.84	4759.01	67,470.04	1166.33	22,924.89	3.73

It can be seen that through the complementary coordination of cascade hydropower and photovoltaics, under the same grid constraints, the expected consumption of the complementary system under this model increases by 863.2 MW·h, in which the consumption of photovoltaic group 1 increases by 1035.7 MW·h, and the consumption of photovoltaic group 2 decreases by 172.5 MW·h. The reasons for this are as follows: Under the cascade minimum water consumption model, due to the difference in power generation characteristics between hydropower plants, hydropower plant 1 is located in upstream, and due to the cascade effect, the power generation per unit of water is more; thus, it will increase its output compared with the model in this paper, and to a certain extent, the sending channel of photovoltaic group 1 in the same zone will be squeezed, resulting in a decrease in the consumption of photovoltaic group 1. Accordingly, the output of hydropower plant 2 is reduced, which makes the absorption of photovoltaic group 2 increase. An analysis found that after carrying out the complementarity of terrace hydropower and PVs, the water consumption increased by 5.784 million m^3, with an unchanged amount of terrace hydropower generation, and the rate of water consumption increased accordingly, which brought certain impacts to the economic operation of terrace hydropower, and it is necessary to further study the mechanism of benefit distributions among hydropower plants under the mode of water–photovoltaic complementarity.

4. Conclusions

This paper presents a short-term optimal scheduling model to maximize the amount of power that can be consumed by a cascade water–photovoltaic complementary system, in order to provide decision support for the operation and scheduling of complementary systems. Through modeling and example analyses, the innovative results and conclusions are as follows:

(1) A refined model maximizes expected power consumption, using units as the smallest scheduling unit, improving detail over traditional hydropower plant-level models. It captures unit-specific characteristics like climbing abilities, vibration zones, starts/stops, and grid zones, aligning better with actual scheduling needs.

(2) Coding methods were fused and innovated to enhance solving efficiency. The unit-level modeling increases solution complexity, so piecewise linear approximations, 0–1 integer variables, power generation head discretization, and other linearization techniques were adapted. This transformed the original MINLP and MILP models for quick, accurate solutions using commercial tools.

(3) The expected model of short-term maximum absorbable power established in this paper can effectively improve the overall absorbable power of the complementary system. However, limited by the physical grid and the hydraulic and electrical

constraints of cascade hydropower, the promotion capacity is limited under the guarantee of the power supply support capacity of the grid.

Considering the multi-subject nature and large demand differences in cascade water–photovoltaic complementary system scheduling, future research should focus on developing a multi-objective coordinated scheduling model and should explore benefit distribution mechanisms among hydropower plants in complementary mode. However, these efforts must account for the practical constraints identified in this study, such as grid limitations and hydropower constraints, to ensure feasible and impactful solutions.

Author Contributions: Conceptualization, J.M. and S.H.; methodology, L.Z.; supervision, Y.W., F.M. and J.W.; writing—original draft, C.W.; writing—review and editing, X.Z.; validation, B.Z. All authors have read and agreed to the published version of the manuscript.

Funding: This research was funded by the Research Project of the National Petroleum and Natural Gas Pipeline Network Group Co., Ltd., "Research on Comprehensive Application Technology of Photovoltaic Power Generation in Oil and Gas Storage and Transportation Engineering", grant number: DTXNY202202. We also greatly appreciate the helpful suggestions and comments of editors and reviewers.

Data Availability Statement: Data are contained within the article.

Conflicts of Interest: Authors Shuzhe Hu, Jingyang Wu, Yue Wang, Chao Wei and Xiaoqin Zhang were employed by the company China Oil & Gas Piping Network Corporation. Author Jinniu Miao and Liqian Zhao were employed by the company China Petroleum Pipeline Engineering Corporation. Author Fanyan Meng was employed by the company China Petroleum Pipeline Research Institute Co., Ltd. The remaining authors declare that the research was conducted in the absence of any commercial or financial relationships that could be construed as a potential conflict of interest. The China Oil & Gas Piping Network Corporation, China Petroleum Pipeline Engineering Corporation and China Petroleum Pipeline Research Institute Co., Ltd. had no role in the design of the study; in the collection, analyses, or interpretation of data; in the writing of the manuscript, or in the decision to publish the results.

Nomenclature

Abbreviation	Description
Hydro	Hydropower
MINLP	Mixed-integer nonlinear programming
MILP	Mixed-integer linear programming
Prob	Probability
WT	Wind turbine
PV	Photovoltaic
OHF	Output–head–flow

Appendix A

Algorithm Coding Example

```
//Introducing the CPLEX solver class in the Java environment
import ilog.concert.IloException;
import ilog.concert.IloNumVar;
import ilog.concert.IloNumVarType;
import ilog.cplex.IloCplex;
public class MyTest {
/**
* obj = x1 + 5 × 2 + x3
* −x1 + x2 + x3 <= 56;
```

```
* x1 − 3 × 2 + x3 <= 39;
* 0 <= x1 <= 40;
* x2 ≥ 0;
* x3 ≥ 0;
*/
public static void main(String[] args) throws IloException {
//Create a new solution model
IloCplex cplex = new IloCplex();
//Variable declaration, 3 variables
int varNum = 3;
IloNumVar [] vars = new IloNumVar[varNum];
Double[] xishu = new double[]{1,5,1};
Double[] mins = new double[]{0,0,0};
Double[] maxs = new double[]{30, Double.MAX_VALUE, Double.MAX_VALUE};
for (int i = 0; i < vars.length; i++){
vars[i] = cplex.numVar(mins[i], maxs[i], IloNumVarType.Float);
}
//Objective function
cplex.addMaximize(cplex.scalProd(vars, xishu));
//Constraints handling
cplex. addLe(cplex. Sum(cplex. prod(1.0, vars [0]), cplex. prod(1.0, vars [1]), cplex. prod(1.0, vars
[2])), 56);
cplex. addLe(cplex. sum(cplex. prod(1.0, vars [0]), cplex. prod(−3.0, vars [1]), cplex. prod(1.0, vars
[2])), 39);
//Model solving
if(cplex.solve()){
cplex.output().println("Solution status = " + cplex.getStatus());
cplex.output().println("Solution value = " + cplex.getObjValue());
//Output variable results
double[] vals = cplex.getValues(vars);
for (int i = 0; i < vals.length; i++){
System.out.println("i: "+i+", value: "+vals[i]);
}
}
cplex.end();
}
}
```

References

1. Janak, J. Do renewable portfolio standards increase renewable energy capacity? Evidence from the United States. *J. Environ. Manag.* **2021**, *287*, 112261. [CrossRef]
2. Weschenfelder, F.; Leite, G.N.P.; Costa, A.C.A.; Vilela, O.C.; Ribeiro, C.M.; Ochoa, A.A.V.; Araújo, A.M. A review on the complementarity between grid-connected solar and wind power systems. *J. Clean. Prod.* **2020**, *257*, 120617. [CrossRef]
3. Zhang, J.T.; Cheng, C.T.; Yu, S.; Shen, J.J.; Wu, X.Y.; Su, H.Y. Preliminary feasibility analysis for remaking the function of cascade hydropower stations to enhance hydropower flexibility: A case study in China. *Energy* **2022**, *260*, 125163. [CrossRef]
4. Wang, X.; Wang, P.F.; Deng, Y.; Xing, X.L.; Yuan, Q.S.; Du, C.G.; Gan, J.W.; Zheng, Y.R.; Liu, Y.X.; Xia, Y.F.; et al. Impacts of cascade hydropower development on river ecosystem homeostasis: A review. *J. Hydrol.* **2024**, *638*, 131484. [CrossRef]
5. Yang, Z.K.; Liu, P.; Cheng, L.; Liu, D.L.; Ming, B.; Li, H.; Xia, Q. Sizing utility-scale photovoltaic power generation for integration into a hydropower plant considering the effects of climate change: A case study in the Longyangxia of China. *Energy* **2021**, *236*, 121519. [CrossRef]
6. Zhang, Y.S.; Ma, C.; Lian, J.J.; Pang, X.L.; Qiao, Y.N.; Chaima, E. Optimal photovoltaic capacity of large-scale hydro-photovoltaic complementary systems considering electricity delivery demand and reservoir characteristics. *Energy Convers. Manag.* **2019**, *195*, 597–608. [CrossRef]
7. Shen, J.J.; Wang, Y.; Cheng, C.T.; Li, X.F.; Miao, S.M.; Zhang, Y.; Zhang, J.T. Research status and prospect of generation scheduling for hydropower-wind-solar energy complementary system. *Proc. CSEE* **2022**, *42*, 3871–3885. [CrossRef]

8. Liu, S.Y.; Wang, J.X.; Li, Q.T.; Wang, X.L.; Liu, Z.T.; Wang, X.B.; Wang, R.G. Optimal configuration of multi-energy complementary composite power plant and its application in generation expansion planning. *Power Syst. Technol.* **2021**, *45*, 3006–3015. [CrossRef]
9. Wang, K.; Wu, X.; Wang, X.; Dang, P. Two-stage stochastic optimal scheduling for multi-microgrid networks with natural gas blending with hydrogen and low carbon incentive under uncertain environment. *J. Energy Storage* **2023**, *72*, 108319. [CrossRef]
10. Luo, B.; Miao, S.M.; Qiu, Y.W.; Gao, L.; Chen, G.; Wang, L. Operation safety analysis method for cascaded hydro-photovoltaic complementary generation system and its application. *Sichuan Electr. Power Technol.* **2021**, *44*, 1–6. [CrossRef]
11. Ming, B.; Li, Y.; Liu, P.; Wang, Y.M.; Ma, C.H.; Huang, Q. Long-term optimal operation of hydro-solar hybrid energy systems nested with short-term energy curtailment risk. *J. Hydraul. Eng.* **2021**, *56*, 712–722. [CrossRef]
12. Yuan, W.N.; Huang, X.F.; Xian, Y.H.C.; Li, D.C.; Li, X. Compensation benefit sharing of hydro-photovoltaic complementary energy based on CRITIC-TOPSIS method. *Power Syst. Technol.* **2024**, *48*, 2003–2011. [CrossRef]
13. Ming, B.; Liu, P.; Guo, S.; Cheng, L.; Zhou, Y.; Gao, S.; Li, H. Robust hydroelectric unit commitment considering integration of large-scale photovoltaic power: A case study in China. *Appl. Energy* **2018**, *228*, 1341–1352. [CrossRef]
14. Zhu, Y.M.; Chen, S.J.; Ma, G.W.; Han, X.Y.; Wang, L. Short-term complementary operation of hydro-photovoltaic integrated system considering power generation and output fluctuation. *Trans. China Electrotech. Soc.* **2020**, *35*, 2769–2779.
15. Luo, B.; Chen, Y.C.; Liu, Z.W.; Miao, S.M.; Wang, H.R.; Zhang, H. Short-term Optimal Dispatch Model for Maximizing Expectation of Accommodation Power of Cascade Hydro-Photovoltaic Complementary System. *Autom. Electr. Power Syst.* **2023**, *47*, 66–75. [CrossRef]
16. Shen, J.J.; Cheng, C.T.; Cao, R.; Lu, J.Y. Key issues and development in large-scale hydropower absorption and peak regulation. *Autom. Electr. Power Syst.* **2018**, *42*, 174–183. [CrossRef]
17. Miao, S.M.; Luo, B.; Liu, B.X.; Shen, J.J.; Cheng, C.T. Short-term coordination model for large and small hydropower consumption considering economy and reliability. *Autom. Electr. Power Syst.* **2018**, *42*, 101–109. [CrossRef]
18. Xu, F.; Li, L.L.; Chen, Z.X.; Tu, M.F.; Ding, Q. Generation scheduling model and application with fluctuation reduction of unit output. *Autom. Electr. Power Syst.* **2012**, *36*, 45–50.
19. Zhong, H.Y.; Huang, Q.; Ming, B.; Liu, P.; Yang, Y.; Wang, Z. An efficient method for deriving reservoir operating rules by coupling ensemble forecasting information. *J. Hydroelectr. Eng.* **2021**, *40*, 44–55. [CrossRef]
20. Cheng, C.T. Function remolding of hydropower systems for carbon neutral and its key problems. *Autom. Electr. Power Syst.* **2021**, *45*, 29–36. [CrossRef]
21. Su, C.G.; Wang, P.L.; Wu, X.Y.; Cheng, C.T.; Wang, J.Y. A compact MILP model for short-term peak shaving of cascaded hydropower plants considering unit commitment. *Power Syst. Technol.* **2018**, *42*, 1883–1891. [CrossRef]
22. Shen, J.J.; Cheng, C.T.; Cheng, X.; Lund, J.R. Coordinated operations of large-scale UHVDC hydropower and conventional hydro energies about regional power grid. *Energy* **2016**, *95*, 433–446. [CrossRef]
23. Su, C.G.; Cheng, C.T.; Wang, P.L.; Shen, J.J.; Wu, X.Y. Optimization model for long-distance integrated transmission of wind farms and pumped-storage hydropower plants. *Appl. Energy* **2019**, *242*, 285–293. [CrossRef]
24. Cheng, C.T.; Wu, X.Y.; Shen, J.J.; Liao, S.L. Short-term optimal operation methods of large-scale hydropower plants I: General overview. *J. Hydraul. Eng.* **2011**, *42*, 1017–1024. [CrossRef]
25. Zhao, Y.Z.; Tang, J.; Wang, J.; Wang, J.; Qiu, M.Q. Study on the operating condition diagnosis method of hydropower station equipment based on fuzzy clustering analysis. *J. Phys.* **2022**, *2303*, 012079. [CrossRef]

Disclaimer/Publisher's Note: The statements, opinions and data contained in all publications are solely those of the individual author(s) and contributor(s) and not of MDPI and/or the editor(s). MDPI and/or the editor(s) disclaim responsibility for any injury to people or property resulting from any ideas, methods, instructions or products referred to in the content.